Electrochimica Acta 398 (2021) 139318

Contents lists available at ScienceDirect

Electrochimica Acta

journal homepage: www.elsevier.com/locate/electacta

Glycerol electro-oxidation at Pt in alkaline media: influence of mass transport and cations

Gabriel Melle[a,b], Matheus B.C. de Souza[c], Patricia V.B. Santiago[c,e], Patricia Gon Corradini[a,d], Lucia Helena Mascaro[a,e], Pablo S. Fernández[c,e], Elton Sitta[a,e,*]

[a] Department of Chemistry, Federal University of Sao Carlos, Rod. Washington Luis, km 235, Sao Carlos, SP 13565-905, Brazil
[b] Instituto de Electroquímica, Universidad de Alicante, Apdo. 99, Alicante E-03080, Spain
[c] Institute of Chemistry, States University of Campinas (UNICAMP), Campinas, SP 13083-970, Brazil
[d] Fluminense Federal Institute of Education, Science and Technology, Campus Itaperuna, Itaperuna, RJ, 28300-000, Brazil
[e] Center for Innovation on New Energies (CINE), Campinas, SP 13083-841, Brazil

ARTICLE INFO

Article history:
Received 23 July 2021
Revised 22 September 2021
Accepted 23 September 2021
Available online 28 September 2021

Keywords:
Glycerol electro-oxidation
Platinum
Cation effect
Oscillation
Mass-transport

ABSTRACT

Glycerol is an important biomass-derived product with potential to be applied on energy converting systems or as platform molecule in electrosynthesis. In this work we studied the glycerol oxidation reaction (GOR) in alkaline media containing distinct alkaline cations and controlling the mass transport. The cyclic voltammograms were deconvoluted into three processes and the changes in the charge of each process revealed that mass transport affects the GOR in a complex matter, depending on both applied potential and electrolyte cation. Regardless of the cation on supporting electrolyte, high-performance liquid chromatography (HPLC) analysis revealed the production of glycerate and lactate during GOR. Finally, potential oscillations under current control were mapped, highlighting the influence of both cations and mass transport, even in the systems with very similar behavior under potential control.

1. Introduction

The glycerol oxidation reaction (GOR) has been gaining prominence in the literature for its wide applicability as energy source and as a precursor of compounds for the pharmaceutical industry [1–4]. The complete glycerol electrochemical conversion, to CO_2, provides 14 electrons (r1):

$$CH_2OH - CHOH - CH_2OH + 14\,OH^- \rightarrow 3\,CO_2 + 11\,H_2O + 14\,e^- \quad (r1)$$

Although it is thermodynamically favorable to use glycerol to feed direct alcohol fuel cells (DAFC) anodes, the total conversion to CO_2 is still a challenge at low temperature DAFC [5]. In practice, partially oxidized species such as aldehydes, ketones and carboxylic acids are the most common GOR products, which could also be an interesting reaction pathway as some of these products are important substances for the chemical industry [6,7]. In this scenario, fundamental studies are valuable for the understanding of the GOR selectivity and future application in industrial processes [6].

The GOR selectivity is deeply affected by the catalyst nature [5,8,9], surface orientation [10–12], and electrolyte pH [2]. We showed that the mass transport also strongly affects the GOR catalyzed by Pt in acidic media [13]. In stagnant electrolyte, partially-oxidized glycerol products, such as glyceraldehyde, can be converted into CO_{ad} and 2C species. However, under facilitated mass transport conditions, these species can be transported to the bulk, diminishing the poisoning and maintaining the surface active for glycerol oxidation. Similar behavior was found on GOR catalyzed by carbon-supported PtSb nanoparticles, in which the mass transport was modulated by the carbon support geometry e.g. CMK-3, CMK-5 or Vulcan [14].

In alkaline media, the supporting electrolyte cation may influence on the overall reaction. Examples of cation-dependence of Pt catalyzed reactions can be found during O_2 [15] and H_2O_2 [16] electroreduction reactions as well as during the CO_{ad} [17], methanol [15], formate [18], ethanol[19] and ethylene glycol [20,21] electro-oxidation reactions. Angelucci et al.[22] showed that the currents at $E > 0.50$ V vs reversible hydrogen electrode (RHE) in cyclic voltammograms (CV) during GOR on Pt increase with the ionic cation radius of electrolytes composed of MOH (M = K, Na, or Li). Strmcnik et al. [15] explained this phenomenon in terms of the stabilization of OH_{ad}-$M(OH)_x$ clusters in which OH_{ad} represents the adsorbed hydroxyl and $M(OH)_x$ the hydrated

* Corresponding author at: Department of Chemistry, Federal University of Sao Carlos, Rod. Washington Luis, km 235, Sao Carlos, SP 13565-905, Brazil.
E-mail address: esitta@ufscar.br (E. Sitta).

https://doi.org/10.1016/j.electacta.2021.139318
0013-4686/

cation. Small cations turn the OH_{ad}-M interaction more effective, stabilizing the adsorbed OH_{ad} at a lower potential and making the adsorption of organic species more difficult, similarly to the effect caused by anions in acidic electrolytes. Moreover, more than a mere surface blocker, the adsorbed cations disturb the double layer and modify the proton-electron transfer dynamics [1,23]. For instance, Sitta et al. [24] showed that alkaline cations can modify the ethylene glycol reaction selectivity, demonstrating that as more blocked the surface is, the lower the occurrence of C-C cleavage, to yield carbonate as a final product.

Rus et al. [25] showed that methanol electro-oxidation reaction is limited by mass transport at low hydroxyl ion concentration, while the electro-catalysis is inhibited by hydroxyl adsorption at high concentrations. This important role of hydroxyl adsorption on surface can also modify the glycerol products re-adsorption, as shown for GOR on Au in alkaline media [26,27]. Herein, we studied the effect of mass transport during GOR catalyzed by Pt in alkaline media composed of distinct alkaline cations under both potential and current controls. The CV was deconvoluted and the peaks were correlated to distinct interactions between glycerol and Pt catalyst. Soluble reaction products were analyzed employing high-performance liquid chromatography (HPLC) and dynamic instabilities were mapped and discussed in terms of changes caused by the cations on the interface during GOR. These results allow us to show that glycerol dynamics at the Pt interface depends on both the mass transport and cations from supporting electrolyte.

2. Experimental

A conventional three electrodes electrochemical cell was used to perform the experiments. The counter electrode (CE) was a platinized platinum mesh, the potential reference was a reversible hydrogen electrode (RHE) prepared with the identical supporting electrolyte solution and the working electrode (WE) was a platinum cylinder embedded in Teflon® yielding 0.2 cm^2 of circular area. Rotation speed (ω) was controlled by a Princeton Applied Research rotating electrode system. The glassware cleanness procedure is described in Ref. [28,29].

The electrochemical surface area was estimated by the charge of hydrogen desorption from underpotential deposition (UPD) region, considering 210 $\mu C\ cm^{-2}$ [30]. All the solutions were prepared by the dissolution of high-pure lithium, sodium or potassium hydroxides (Sigma-Aldrich 99.95%, metal grade) and glycerol (Sigma-Aldrich, > 99% GC) in ultra-pure water (Millipore, 18.2 MΩ cm). All chemicals were used as received. Distinct amounts of MOH (M = Li, Na, or K) were dissolved in ultra-pure water to yield 0.50 mol L^{-1} solutions and used as a supporting electrolyte. Glycerol was directly added into solutions yielding 0.10 mol L^{-1}. The solutions were purged with Argon (White Martins, 5.0 N) for at least 20 min and, during the experiment, the Argon flow was maintained in the cell's headspace. The system cleanness was monitored by taking the Pt CV profiles from 0.05 to 1.30 V at 0.10 V s^{-1}[18] in the absence of glycerol, (Fig. S1 of the supplementary information (SI) section).

All experiments were performed at room temperature (25 ± 2 °C) and controlled by an Autolab 128N potentiostat/galvanostat equipped with Scan250 modulus. Deconvolution analysis was performed using the statistical method to fit the peaks based on the Gaussian distribution. Adjustments to deconvoluted curves were applied to obtain $\chi^2 > 0.99$.

Samples for the HPLC analysis were collected using a Shimadzu sample collector FRC-10A while performing a linear sweep voltammetry at 1 mV s^{-1} on a platinum disk with 0.9 cm diameter as WE. The samples were acquired at a flow rate of 0.06 mL min^{-1} by placing a peek capillary tip close to surface of the WE, held in place by a Teflon holder. The experimental setup is described in references [2,31] and shown in Fig. S2). Each sample corresponds to a 60 mV potential interval during the potential sweep, and were stored in 0.5 mL plastic tubes (Eppendorf) containing 10 μL of a 1.5 mol L^{-1} H_2SO_4 solution, in order to reduce the sample's pH to 3.30, avoiding undesired side reactions [32].

The HPLC analysis was performed in a Shimadzu LC-6AD chromatograph using both a refractory index and *UV-vis* detectors. The mobile phase was a 0.5 mmol L^{-1} H_2SO_4 solution with a flow rate of 0.06 mL min^{-1}, with an injection volume of 20 μL. Three columns were used in series: an Aminex HPX-87H followed by two Shodex Sugar SH1011, all kept at 84ºC in a column oven, and preceded by an Aminex micro-guard cation H cartridge.

3. Results

Fig. 1 shows the CV behavior for GOR in LiOH (a), NaOH (b), and KOH (c) solutions at distinct electrode rotation speeds (ω) from 0 (stagnant electrolyte) to 1600 rpm. Positive and negative-going scans are represented by the continuous and dashed lines, respectively. For LiOH electrolyte (Fig. 1(a)) during a positive-going scan, it is discernible three current peaks centered at 0.70, 0.75, and 1.10 V named I, II, and III, respectively, and during a negative-going scan, two current peaks, IV and V, are observed at 1.10 and 0.60 V, respectively.

Fig. 1 also presents the deconvoluted three peaks observed on positive-going scan and the correspondence between the sum of these deconvoluted peaks and the experimental curves (dashed line) for LiOH (a2), NaOH (b2), and KOH (c2) at 400 rpm. In the presence of Na^+ or K^+ ions, the peaks I and II are less highlighted than in LiOH solutions, however, applying the deconvolution procedure it is possible to isolate the processes I and II in all three supporting electrolytes.

The effect of ω on the GOR is shown in Fig. 2 in terms of the charge (q) of each deconvoluted peak on a positive-going scan. For the LiOH electrolyte, the charge slightly increases on both peak I and II with ω, however, the opposite effect is observed on peak III. For the NaOH and KOH electrolytes, while the charge of peak I substantially increase with ω, a slight decrease on peaks II and III are observed, indicating that the processes occurring at peak I are the main responsible for the overall increase in the activity from NaOH to KOH supporting electrolytes.

We also performed HPLC analysis from samples collected near the WE surface at 1 mV s^{-1}. The chromatograms used to identify the products as well as the calibration curves are shown on Figs. S3–S5 in SI files section. Fig. 3 shows that, regardless the cation electrolyte, glycerate and lactate were observed as soluble products at potentials higher than 0.6 V. We normalized the signals based on maximum glycerate production in each experiment and the error bars represent the standard deviation obtained from the mean value of three experiments. Small amounts of glycolate were also detected, however, their quantification was difficult due to its production being near the detection limit of our equipment (its highest concentration detected was in the order of 5 μmol L^{-1}). The carbonate production cannot be detected by HPLC, but we have already reported the complete oxidation of glycerol in previous publications [8,9]. In these works, it is shown that there is a reaction pathway in which the polyol adsorbs at the Pt surface yielding CO_{ad}, which is further oxidized to carbonate.

When the GOR is performed under current instead of potential control, potential oscillations can be observed in both acidic and alkaline media [33,34]. Fig. 4(a1, b1, and c1) presents galvanodynamic curves, at 7.5 μA cm^{-2} s^{-1}, showing the potential behavior at distinct ω and supporting electrolytes. Regardless of the supporting electrolyte employed, it was observed a rapid potential increase in small current densities at potentials below 0.50 V followed by a slow potential evolution from ca 0.50 V to ca 0.75 V,

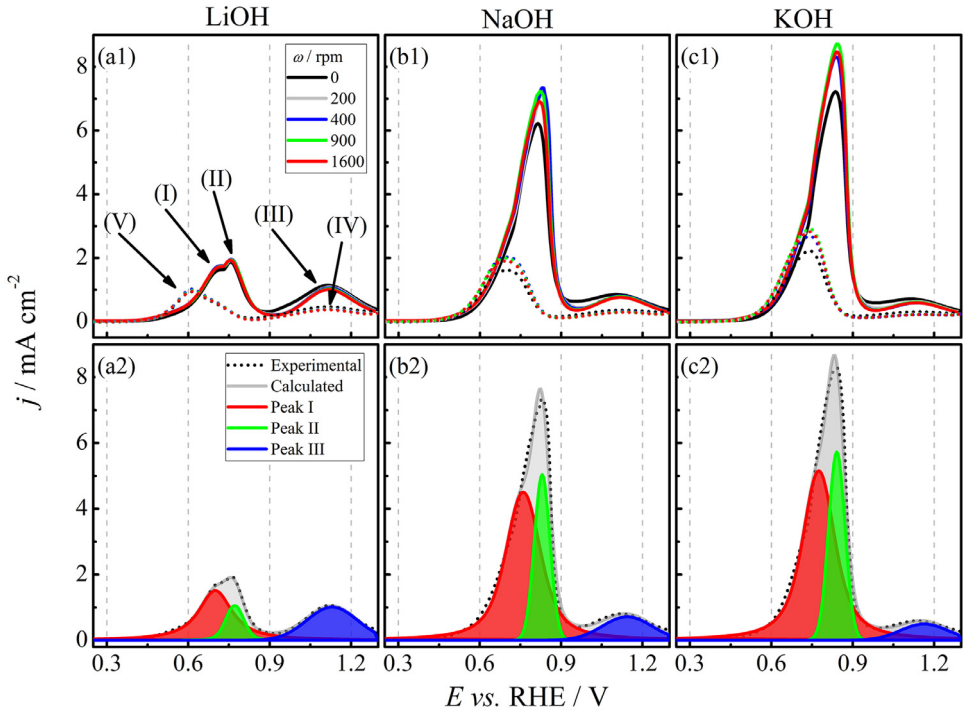

Fig. 1. Pt cyclic voltammograms (CV) at 0.10 V s^{-1}.in 0.1 mol L^{-1} of glycerol and 0.5 mol L^{-1} of (a1) LiOH, (b1) NaOH, or (c1) KOH for several rotation speeds. Full and dashed lines correspond to the positive and negative sweep, respectively. Deconvolutions for cyclic voltammograms obtained at 400 rpm in (a2) LiOH, (b2) NaOH, or (c2) KOH.

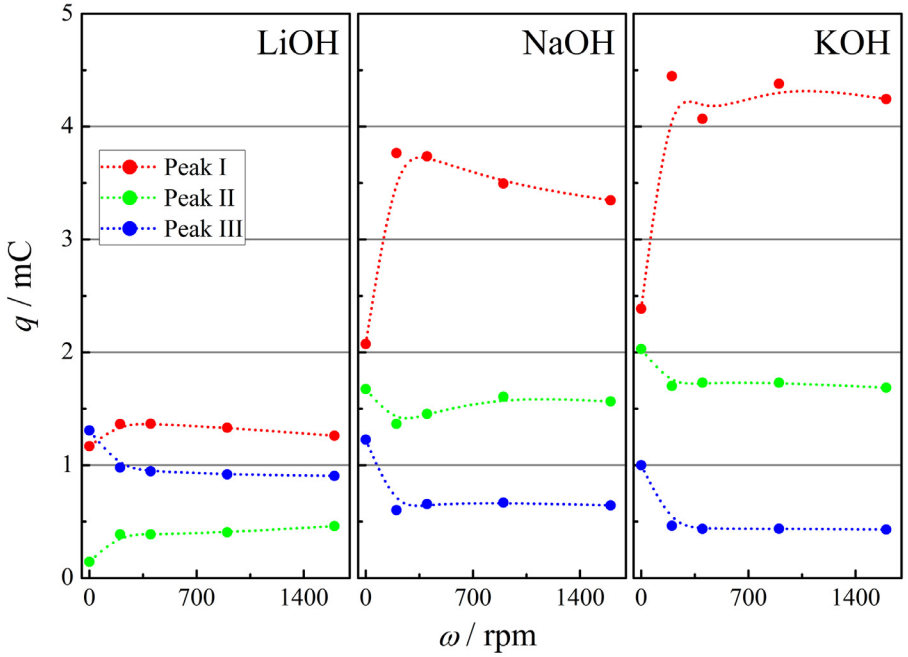

Fig. 2. Charges of Peak I, II, and III observed for CV experiments (Fig. 1) at distinct ω, in LiOH, NaOH, and KOH electrolytes.

in agreement with the potential region in which GOR occurs in CV. At this point, the potential can fast increase to $E>$ 1.20 V or oscillate from 0.75 to 0.30 V. While for LiOH electrolyte, regardless ω, the system does not show potential oscillations, this phenomenon is observed in quiescent solution ($\omega = 0$) for both NaOH and KOH electrolytes. The GOR oscillations in KOH agree with the literature [33,35].

Interestingly, increasing ω, the current necessary for the potential to jump to $E>$ 1.20 V decreases, this behavior not being directly related to the charges changes of peaks I and II with ω. Galvanostatic time-series were also collected at currents near the potential jump to $E>$ 1.20 V for each supporting electrolyte in galvanodynamic curves. This normalization procedure described in ref. [36] has been used to compare oscillations in distinct experimental conditions. Moreover, experiments at constant current allow us to analyze the potential evolution along the time. The time-series are also shown in Fig. 4(a2, b2, and c2).

Again, in LiOH electrolyte no oscillatory behavior was found during GOR, even applying the current normalization, the time-series length (time demanded to the potential jump to $E >$ 1.20 V)

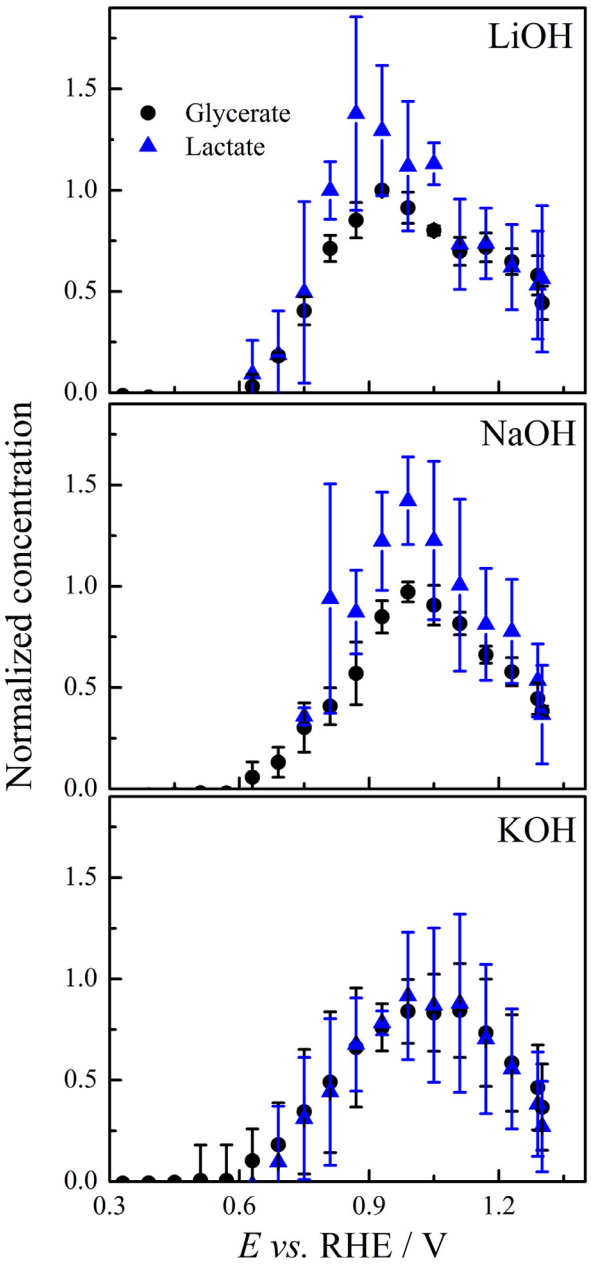

Fig. 3. Reaction products quantified by HPLC analysis, as function of potential for GOR in the same experimental condition of Fig. 1. Scan rate 1 mV s^{-1}.

decreases with rotation speed. On the other hand, besides the decrease of time-series length, the electrode rotation modifies the oscillatory behavior of GOR in both NaOH and KOH. While in NaOH the oscillations were completely suppressed by the mass-transport in conditions as low as 200 rpm, in KOH these oscillations were maintained from 0 to 1600 rpm. Besides, it is worth noticing that the oscillation patterns also depend on the mass-transport as discussed in the sequence.

Fig. 5 shows the oscillations patterns (column (a)) observed during galvanostatic (j = 1.75 mA cm^{-2}) GOR in stagnant KOH solutions (Fig. 4(c2). After a 130 s induction period in which the potential increase until reaching ca 0.75 V, harmonic period 1 (P1S) oscillations (Fig. 5(a1)) with an oscillation frequency of 4.8 Hz (see analysis on Fig. S6) and small potential amplitude (from 0.70 to 0.77 V) are observed during ca 25 s. The returned map [37] of this pattern is shown in Fig. 5(b1) confirming its stability and a slow potential increase along the time-series. The oscillations evolve to a period 2 (P2) pattern (Fig. 5(a2)) and then to a nonperiodic pattern that can be divided into two regions: first, a window with small amplitude (lower than 0.15 V) oscillations named Sx, shown on Fig. 5(a3), and a second window characterized by pattern composed by a small amplitude set of oscillations, followed by a sharp high-amplitude peak (Fig. 5(a4)). The last pattern seems to correspond to the mixed-mode oscillations (Px). The return maps are shown in Fig. 5(b2), (b3), and (b4) correspond to the oscillations P2, Sx, and Px, respectively and they clearly show the transition from P1 to P2 through the map divided into two groups as well as the nonperiodic nature of oscillations of both Sx and Px. Oscillations patterns with their return maps for galvanostatic GOR in non-stagnant KOH solutions are described on Fig. S7.

4. Discussion

The HPLC analysis revealed the same GOR soluble oxidation products in the three supporting electrolytes employed. The presence of these products suggests that both primary and secondary alcohol groups on the glycerol molecule can be oxidized to glyceraldehyde and di-hydroxyacetone (DHA), respectively. These species are in equilibrium in alkaline media, but DHA can undergo chemical reactions yielding lactate. Although unstable in alkaline media, glyceraldehyde could be also electrochemically oxidized to glycerate. Alternatively, glycerate could be produced by the (unlikely) directed transfer of 4 electrons. Scheme 1 summarizes the proposed pathways to yield the species identified on HPLC. Dotted and solid arrows correspond to chemical and electrochemical steps, respectively.

Pt in alkaline media has a low activity for the electro-oxidation of both glycerate [8] and lactate [38], thus these species are final products instead of soluble intermediates. Interestingly, the GOR in acidic media strongly depends on the presence of glyceraldehyde near the interface [13], which makes the reaction highly sensitive to mass transport. In our previous work about mass transport effect during GOR, in acidic media, it was suggested a simple reaction scheme based on an intermediate that can diffuse to solution or be consumed on the interface. Numerical simulations indicated that this reaction scheme leads to the increase followed by a slight decrease of peak I. In alkaline media, similar reaction scheme could be applied, however, herein, we observed a much more moderated effect of the mass transport on CV profiles. We hypothesize that it could be connected to a much smaller concentration of the aldehyde near the surface in alkaline media due to the continuous disappearance as a consequence of its chemical transformation into the low-reactive glycerate and lactate (Scheme 1).

The correlation between the current peaks and the products observed in HPLC is not trivial, mainly because we are working near the equipment detection limit and, as aforementioned, some products such as carbonate from CO_{ad} oxidation cannot be detected. Besides, it is important to note that, while the current profile corresponds to the derivative of the charge, the quantification is based on product accumulation, for instance, for each supporting electrolyte, glycerate and lactate productions start on the same potential, that corresponds to the peak I region, but their maximum concentration is detected on the potentials between peaks II and III.

Regardless of the cation employed on supporting electrolyte, the peaks I and II correspond to the oxidation of glycerol or glycerol residues on the onset of the Pt-OH_{ad} region, which is commonly described by a Langmuir-Hinshelwood mechanism [39,40]. Derivative analysis (dj/dE - Fig. S8) on the onset of peak I indicate that net positive currents occur around 0.32 V, and that the GOR increases in the sequence Li > Na > K to potentials up to 0.46 V, followed by an inhibitory effect at higher potentials, confirming that the stabilization of oxygenated species promoted by the small

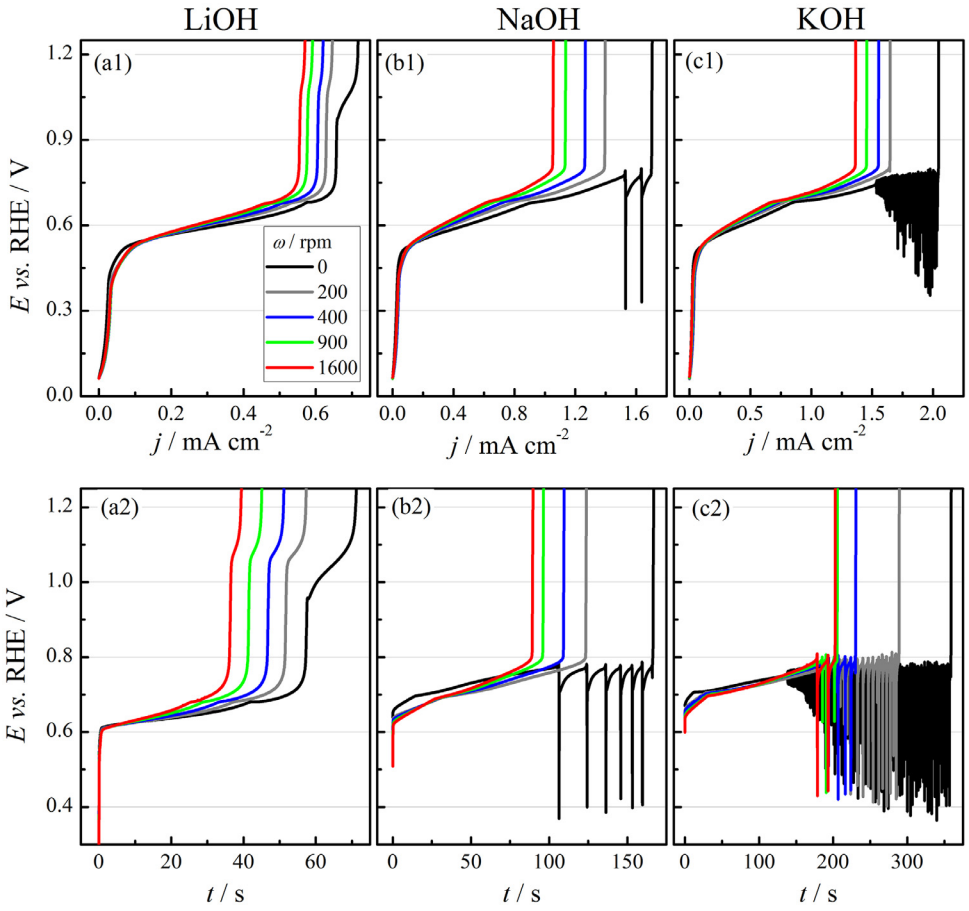

Fig. 4. Galvanodynamic curves at 7.5 μA $cm^{-2}s^{-1}$ (a1, b1 and c1) and galvanostatic time-series (a2, b2 and c2) for Pt disc at distinct ω in solutions of glycerol (0.1 mol L^{-1}) + MOH (0.5 mol L^{-1}) M = Li (a), Na (b) or K (c). Currents employed for each galvanostatic experiment are shown on Table S1.

cations not only catalyzes the oxidation of surface poisons but also inhibits the re-adsorption of new glycerol molecules or other electroactive intermediates [41]. While the cations are able to modify the oxidation current, the selectivity to 3C products seems to be maintained. Thus, these differences might be mainly related to the generation of more oxidized species, for instance, the carbonate. Selectivity changes caused by cation interaction with adsorbed OH_{ad} have origin in the extinguishment of active sites with large number of free Pt sites. Thus, the pathways that demand adsorption by multi-bonded intermediates are more affected by small cations, as was reported for the ethylene glycol electro-oxidation reaction [24]. In this sense, the effect of distinct cations on the Pt-water interface should be more highlighted on the carbonate production during GOR instead of the soluble products detected here using HPLC.

Qualitatively, the dependence of q for each peak with ω is similar for all the electrolytes, however, in the NaOH and KOH electrolytes, the peak I depicts the highest changes with ω, i.e this peak is increased by a factor of at least two when ω increases from 0 to 200 rpm, suggesting the influence of some soluble species. On this potential region, the low interaction between hydrated Na^+ and K^+ with adsorbed oxygenated species could be allowing the intermediates to adsorb, leading to surface poisoning. These observations can be again explained by the re-adsorption of highly unstable species, such as glyceraldehyde. Once glycerate and lactate depict a very low activity on Pt in alkaline media, we hypothesize that the unstable species such as glyceraldehyde could be playing an important role on overall charge observed on CV. The presence of Li^+ inhibits the re-adsorption steps due to their higher interaction with adsorbed oxygenated species on the surface.

The non-covalent interaction between hydrated Na^+ and K^+ ions and the adsorbed oxygenated species increases with the potential, so, by the same reasons that in LiOH solution the peak I slightly changes with mass transport, ω depicts a minor effect on the charge of peaks II and III. However, while the peak II charges follow the same order of peak I, i.e. $q_{Li} < q_{Na} < q_K$, the charges of peak III depict the opposite behavior, providing more charge from the systems containing LiOH than those with NaOH or KOH. The explanation for this trend comes also from the non-covalent interactions between the hydrated cation and $OH_{ad,}$ in which the higher intensity between $Li(H_2O)_x^+$ and OH_{ad} prevents the formation of PtO on the electrode surface. Due to electrostatic repulsion, O_{ad} can undergo place exchange with Pt atoms and become located on the subsurface, decreasing the Pt catalytic activity.

Instabilities in electrochemical systems are connected to the competition between, at least, two feedback loops, that are usually described as an active branch composed of a set of electron donor/receptor processes and an inhibitory branch, formed by poisoning species. The oscillations are very sensitive to the system's initial conditions as well as to small perturbations along the time which is highlighted in the completely distinct behavior between GOR in NaOH and KOH solutions. While in KOH the oscillations are gradually inhibited with ω, similar to the oscillations shown during GOR in acidic media [13], in NaOH they start with a distinct pattern and are extinguished in non-quiescent solutions. Note that CV profiles of GOR in NaOH and KOH solutions, including the peak charges, are quite similar.

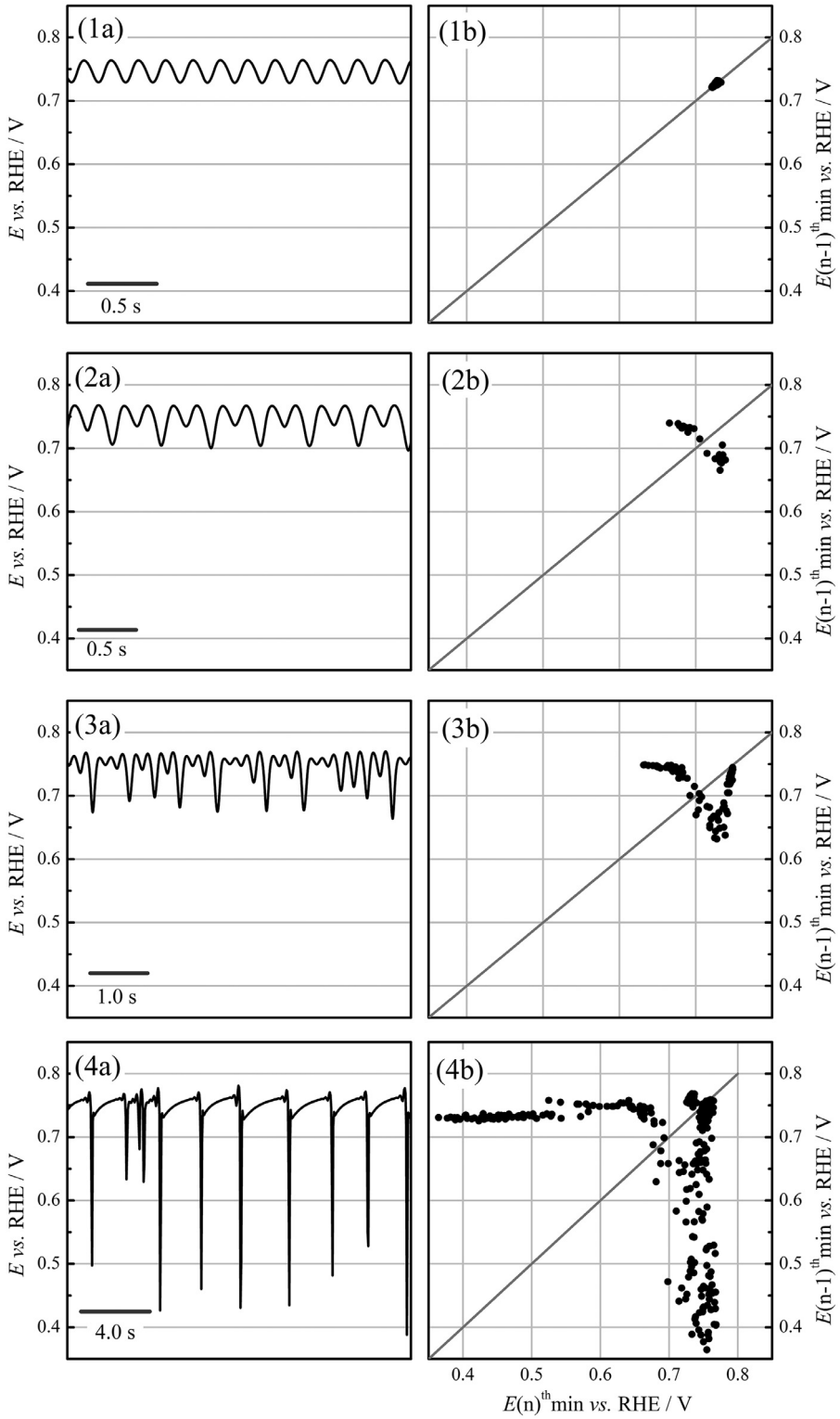

Fig. 5. Oscillation pattern samples obtained during galvanostatic time-series at 1.75 mA cm^{-2} for GOR in KOH electrolyte and $\omega = 0$ (column (a)). Respective return maps for each pattern (column (b)).

P1S, P2 and Sx patterns occur on the potential of peaks I, covering the onset of peak II, likewise, Px pattern spent the most of its time in this potential region with only fast excursions to the low (0.4 V) potential region. In this potential window, the formation of absorbed glycerol residues at low potentials are expected, as well as the soluble products glycerate and lactate according to Scheme 1. It is reported in the literature that the cation interactions with oxygenates adsorbed species modifies the oscillations observed during ethanol [19] and ethylene glycol [20] oxidation reactions on Pt(*poly*). In both cases, higher currents are observed in KOH solution than in NaOH and LiOH solutions, however, the oscillatory behavior is present regardless of the cation on supporting electrolyte.

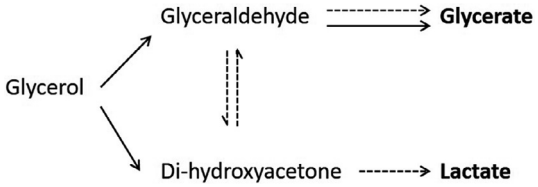

Scheme 1. Proposed reaction pathways for glycerol electrooxidation in alkaline media on Pt based on the products observed using HPLC. Dotted and solid arrows correspond to chemical and electrochemical steps, respectively. The identified products in HPLC are represented in bold.

To take advantage of the high sensitivity of oscillations with experimental conditions, the analysis of oscillation evolution with time is important to infer about the product accumulation on and near the electrode/solution interface. The oscillations during GOR in KOH at $\omega = 0$ follow a common behavior found for other small organic molecules [42–44] that consists in: the induction period to reach the surface/interface conditions (intermediate covering) necessary to oscillations; oscillation birth with simple patterns such as quasi-harmonic period 1 with small amplitude; evolution to more complex patterns with higher amplitude until the potential jump to $E > 1.20$ V. The trend observed in the present work also agrees with Oliveira et al. [33] that mapped the GOR oscillations in 1.0 mol L^{-1} KOH observing the evolution from P1S to more complex systems, but at glycerol concentrations higher than 0.1 M, mixed-mode oscillations dominate the time-series.

At $\omega > 0$ both the time-series length and the patterns are changed. The time-series at 200 rpm (Fig. S7a) does not show the P1S nor P2 patterns and although the induction period increased, the time in which the time-series spend oscillating is 35% lower than the time at $\omega = 0$. Near the onset of oscillations, it is possible to observe some Px with a small amplitude that is quite similar to the Sx, however, this pattern is fast replaced by Px with a large amplitude similar to the patterns in Fig. 5(d). Increasing ω (Fig. S7) this tendency is confirmed, i.e. the oscillations appear in a lower time window and the patterns correspond to those observed at the end of time-series in a stagnating electrolyte. The GOR oscillations in NaOH (Fig. 4(b2)) also correspond to the Px described to the KOH electrolyte.

The decrease of the induction period and the patterns transitions let us presume that the glycerol reactive intermediates play a decisive role in the oscillatory dynamics in the following way: (i) the induction period is necessary for the intermediate accumulation on the surface, providing the conditions for the oscillation starts; (ii) along with the oscillations, part of these accumulated intermediates are consumed when the potential limits are distinct of the induction period, and the reposition (by GOR) is not able to maintain the conditions present on the surface in the onset of oscillations, changing the patterns. It is important to emphasize that slight changes on the surface are necessary to modify the patterns as suggested by numerical simulation [45]; (iii) after the time-series reaches the condition for Px patterns, the systems are no longer able to provide the number of electrons imposed by the galvanostatic condition and the potential jump to $E > 1.20$ V. Increasing ω, in KOH, causes the removal of these intermediates and the surface condition becomes similar to the stagnant electrolyte after the oscillation evolution, i.e., Px patterns and the potential jump to $E > 1.20$ V. Replacing KOH by NaOH, the oscillations have already the Px pattern in stagnant electrolyte letting the convective mass-transport to extinguish the oscillations.

The model described above is very sensitive to the system conditions, for instance, Oliveira et al. [33] found that the majority of the oscillations depict Px patterns for several current values in galvanostatic time-series with glycerol concentrations higher than 0.1 M. Zulke et al. [35] also described that the oscillations during GOR were extinct for $\omega > 0$ in 0.1 mol L^{-1} KOH and glycerol concentration of 0.30 mol L^{-1}.

5. Conclusions

We described the effect of both alkaline cation and mass-transport on the glycerol oxidation reaction (GOR) in alkaline media. The main conclusions are addressed below:

- Regardless of the cation present in the supporting electrolyte, it is possible to deconvolute the cyclic voltammograms in three peaks during a positive-going scan and two peaks during a negative-going scan. In quiescent electrolytes, the charge of the peaks I and II follow the order: qLi < qNa < qK, the opposite being observed at the peak III. While the three peaks on LiOH electrolyte slightly depends on the mass transport, in NaOH and KOH electrolytes it is observed a mass transport dependence for peak I.
- The analysis of near interface electrolyte samples revealed the production of glycerate and lactate. Both products are generated through the chemical conversion of glyceraldehyde and di-hydroxyacetone in alkaline media. Besides, glycerate also can be produced by the glyceraldehyde electrochemical oxidation. We hypothesize that, similarly to which was observed in acidic media, GOR in alkaline media involves desorption and re-adsorption of active species, however, these species (probably glyceraldehyde) are highly unstable in alkaline media, yielding lactate and glycerate.
- Oscillations were observed during GOR only in KOH and NaOH, but they are extinguished increasing the mass-transport in the latter case. In KOH, several oscillation patterns were identified, and the increase of mass-transport extinguished the first patterns c.f. period 1 and 2, leading the system to show mixed-mode oscillations. The oscillations extinguishment/modification with mass transport highlight the role of soluble species on GOR in alkaline.

Declaration of Competing Interest

The authors declare that they have no known competing financial interests or personal relationships that could have appeared to influence the work reported in this paper.

Credit authorship contribution statement

Gabriel Melle: Conceptualization, Investigation, Formal analysis. **Matheus B.C. de Souza:** Investigation, Formal analysis. **Patricia V.B. Santiago:** Investigation, Formal analysis. **Patricia Gon Corradini:** Investigation, Formal analysis. **Lucia Helena Mascaro:** Formal analysis. **Pablo S. Fernández:** Formal analysis. **Elton Sitta:** Conceptualization, Formal analysis, Supervision.

Acknowledgment

The authors thank to the Coordenação de Aperfeiçoamento de Pessoal de Nível Superior - Brasil (CAPES) - Finance Code 001 and the Conselho Nacional de Pesquisa e Desenvolvimento (CNPq), for fellowships and grants (#430426/2018-6). The authors also thank the São Paulo Research Foundation (FAPESP) (Grants #2013/07296-2, #2014/50249-8, #2017/11986-5, #2018/20952-0 and #2019/00305-2), Shell, and the strategic importance of the support given by ANP (Brazil's National Oil, Natural Gas and Biofuels Agency) through the R&D levy regulation.

Supplementary materials

Supplementary material associated with this article can be found, in the online version, at doi:10.1016/j.electacta.2021.139318.

References

[1] B. Garlyyev, S. Xue, S. Watzele, D. Scieszka, A.S. Bandarenka, Influence of the nature of the alkali metal cations on the electrical double-layer capacitance of model Pt(111) and Au(111) electrodes, J. Phys. Chem. Lett. 9 (2018) 1927–1930, doi:10.1021/acs.jpclett.8b00610.

[2] Y. Kwon, K.J.P. Schouten, M.T.M. Koper, Mechanism of the catalytic oxidation of glycerol on polycrystalline gold and platinum electrodes, ChemCatChem 3 (2011) 1176–1185, doi:10.1002/cctc.201100023.

[3] D. Strmcnik, K. Kodama, D. van Der Vliet, J. Greeley, V.R. Stamenkovic, N.M. Marković, The role of non-covalent interactions in electrocatalytic fuel-cell reactions on platinum, Nat. Chem. 1 (2009) 466–472, doi:10.1038/nchem.330.

[4] T. Li, D.A. Harrington, An overview of glycerol electrooxidation mechanisms on Pt, Pd and Au, ChemSusChem. 14 (2021) 1472–1495, doi:10.1002/cssc.202002669.

[5] E. Antolini, Glycerol electro-oxidation in alkaline media and alkaline direct glycerol fuel cells, Catalysts 9 (2019) 980, doi:10.3390/catal9120980.

[6] S.A.N.M. Rahim, C.S. Lee, F. Abnisa, M.K. Aroua, W.A.W. Daud, P. Cognet, Y. Pérès, A review of recent developments on kinetics parameters for glycerol electrochemical conversion-a by-product of biodiesel, Sci. Total Environ. 705 (2020) 135137, doi:10.1016/j.scitotenv.2019.135137.

[7] M. Simões, S. Baranton, C. Coutanceau, Electrochemical valorisation of glycerol, ChemSusChem 5 (2012) 2106–2124, doi:10.1002/cssc.201200335.

[8] M.B.C. de Souza, R.A. Vicente, V.Y. Yukuhiro, C.T.G.V.M.T. Pires, W. Cheuquepán, J.L. Bott-Neto, J. Solla-Gullón, P.S. Fernández, Bi-modified Pt electrodes toward glycerol electrooxidation in alkaline solution: effects on activity and selectivity, ACS Catal. 9 (2019) 5104–5110, doi:10.1021/acscatal.9b00190.

[9] M.B.C. de Souza, V.Y. Yukuhiro, R.A. Vicente, C.T.G. Vilela Menegaz Teixeira Pires, J.L. Bott-Neto, P.S. Fernández, Pb- and Bi-modified Pt electrodes toward glycerol electrooxidation in Alkaline Media. Activity, selectivity, and the importance of the Pt atoms arrangement, ACS Catal. 10 (2020) 2131–2137, doi:10.1021/acscatal.9b04805.

[10] V. Del Colle, L.M.S. Nunes, C.A. Angelucci, J.M. Feliu, G. Tremiliosi-Filho, The influence of stepped Pt[n(111)×(110)] electrodes towards glycerol electrooxidation: Electrochemical and FTIR studies, Electrochim. Acta 346 (2020) 136187, doi:10.1016/j.electacta.2020.136187.

[11] J.F. Gomes, F.B.C. de Paula, L.H.S. Gasparotto, G. Tremiliosi-Filho, The influence of the Pt crystalline surface orientation on the glycerol electro-oxidation in acidic media, Electrochim. Acta 76 (2012) 88–93, doi:10.1016/j.electacta.2012.04.144.

[12] R.M.L.M. Sandrini, J.R. Sempionatto, G. Tremiliosi-Filho, E. Herrero, J.M. Feliu, J. Souza-Garcia, C.A. Angelucci, Electrocatalytic oxidation of glycerol on platinum single crystals in Alkaline Media, ChemElectroChem 6 (2019) 4238–4245, doi:10.1002/celc.201900311.

[13] G.B. Melle, E.G. Machado, L.H. Mascaro, E. Sitta, Eff ect of mass transport on the glycerol electro-oxidation, Electrochim. Acta 296 (2019) 972–979, doi:10.1016/j.electacta.2018.11.085.

[14] R.N. de Andrade, N. Perini, J.L. Vieira, J.M.R. Gallo, E. Sitta, Glycerol electrooxidation catalyzed by Pt-Sb supported in periodic mesoporous carbon CMK-3 and CMK-5, J. Electroanal. Chem. 896 (2021) 115158, doi:10.1016/j.jelechem.2021.115158.

[15] D. Strmcnik, K. Kodama, D. van der Vliet, J. Greeley, V.R. Stamenkovic, N.M. Marković, The role of non-covalent interactions in electrocatalytic fuel-cell reactions on platinum, Nat. Chem. 1 (2009) 466–472, doi:10.1038/nchem.330.

[16] K.N. da Silva, R. Nagao, E. Sitta, Alkali cation effect during the oscillatory electroreduction of H_2O_2 on Pt, ChemistrySelect 2 (2017) 11713–11716, doi:10.1002/slct.201702276.

[17] C. Stoffelsma, P. Rodriguez, G. Garcia, N. Garcia-Araez, D. Strmcnik, N.M. Marković, M.T.M. Koper, Promotion of the oxidation of carbon monoxide at stepped platinum single-crystal electrodes in alkaline media by lithium and beryllium cations, J. Am. Chem. Soc. 132 (2010) 16127–16133, doi:10.1021/ja106389k.

[18] B.A.F. Previdello, E.G. Machado, H. Varela, The effect of the alkali metal cation on the electrocatalytic oxidation of formate on platinum, RSC Adv. 4 (2014) 15271–15275, doi:10.1039/C4RA00769G.

[19] L.F. Sallum, A. Mota-Lima, E.R. Gonzalez, Galvano– and Potentio–dynamic studies during ethanol electro-oxidation reaction in acid vs. alkaline media: energy dissipation and blocking nature of potassium, Electrochim. Acta 293 (2019) 247–259, doi:10.1016/j.electacta.2018.09.118.

[20] E. Sitta, R. Nagao, I.Z. Kiss, H. Varela, Impact of the alkali cation on the oscillatory electro-oxidation of ethylene glycol on platinum, J. Phys. Chem. C. 119 (2015) 1464–1472, doi:10.1021/jp5105505.

[21] K.N. da Silva, E. Sitta, Tuning oscillatory time-series evolution by Pt(111)-OHad stabilization, J. Solid State Electrochem. 24 (2020) 1921–1926, doi:10.1007/s10008-020-04557-7.

[22] C.A. Angelucci, H. Varela, G. Tremiliosi-Filho, J.F. Gomes, The significance of non-covalent interactions on the electro-oxidation of alcohols on Pt and Au in alkaline media, Electrochem. Commun. 33 (2013) 10–13, doi:10.1016/j.elecom.2013.03.039.

[23] C. Wildi, G. Cabello, M.E. Zoloff Michoff, P. Vélez, E.P.M. Leiva, J.J. Calvente, R. Andreu, A. Cuesta, Super-nernstian shifts of interfacial proton-coupled electron transfers: origin and effect of noncovalent interactions, J. Phys. Chem. C. 120 (2016) 15586–15592, doi:10.1021/acs.jpcc.5b04560.

[24] E. Sitta, B.C. Batista, H. Varela, The impact of the alkali cation on the mechanism of the electro-oxidation of ethylene glycol on Pt, Chem. Commun. (2011) 47, doi:10.1039/c0cc05353h.

[25] E.D. Rus, R.H. Wakabayashi, H. Wang, H.D. Abruña, Methanol oxidation at platinum in alkaline media: a study of the effects of hydroxide concentration and of mass transport, ChemPhysChem (2021) 202100087 n/acphc, doi:10.1002/cphc.202100087.

[26] X. Shi, D.E. Simpson, D. Roy, The role of chemisorbed hydroxyl species in alkaline electrocatalysis of glycerol on gold, Phys. Chem. Chem. Phys. 17 (2015) 11432–11444, doi:10.1039/C5CP00313J.

[27] L. Pérez-Martínez, L. Balke, A. Cuesta, Reactive and inhibiting species in the electrocatalytic oxidation of glycerol on gold. A study combining *in-situ* visible reflectance and ATR-SEIRAS, J. Catal. 394 (2021) 1–7, doi:10.1016/j.jcat.2020.12.010.

[28] G.B. Melle, F.W. Hartl, H. Varela, E. Sitta, The effect of solution pH on the oscillatory electro-oxidation of methanol, J. Electroanal. Chem. 826 (2018) 164–169, doi:10.1016/j.jelechem.2018.08.033.

[29] I.A. Fiori, G.B. Melle, E. Sitta, Halide adsorption effect on methanol electrooxidation reaction studied by dynamic instabilities, J. Electroanal. Chem. 856 (2020) 113657, doi:10.1016/j.jelechem.2019.113657.

[30] S. Trasatti, O.A. Petrii, Real surface area measurements in electrochemistry, J. Electroanal. Chem. 327 (1992) 353–376, doi:10.1016/0022-0728(92)80162-W.

[31] Y. Kwon, M.T.M. Koper, Combining voltammetry with hplc: application to electro-oxidation of glycerol, Anal. Chem. 82 (2010) 5420–5424, doi:10.1021/ac101058t.

[32] Y.Y. Birdja, M.T.M. Koper, The importance of cannizzaro-type reactions during electrocatalytic reduction of carbon dioxide, J. Am. Chem. Soc. 139 (2017) 2030–2034, doi:10.1021/jacs.6b12008.

[33] C.P. Oliveira, N.V. Lussari, E. Sitta, H. Varela, Oscillatory electro-oxidation of glycerol on platinum, Electrochim. Acta. 85 (2012) 674–679, doi:10.1016/j.electacta.2012.08.087.

[34] Gabriel B. Melle, Thiago Altair, Rafael L. Romano, H. Varela, Electrocatalytic efficiency of the oxidation of ethylene glycol, glycerol, and glucose under oscillatory regime, Energy Fuels 35 (2021) 6202–6209, doi:10.1021/acs.energyfuels.1c00203.

[35] A. Zülke, P. Perroni, E.G. Machado, H. Varela, Rrde studies of glycerol electrooxidation: local pH variation and oscillatory dynamics, ECS Trans. 77 (2017) 1643–1650, doi:10.1149/07711.1643ecst.

[36] R. Nagao, I.R. Epstein, E.R. Gonzalez, H. Varela, Temperature (Over)compensation in an oscillatory surface reaction, J. Phys. Chem. A. 112 (2008) 4617–4624, doi:10.1021/jp801361j.

[37] S.H. (Steven H. author StrogatzNonlinear Dynamics and Chaos : With Applications to Physics, Biology, Chemistry, and Engineering, Perseus Books Publishing, 1994 https://search.library.wisc.edu/catalog/9910223127702121.

[38] D.J. Chadderdon, L. Xin, J. Qi, B. Brady, J.A. Miller, K. Sun, M.J. Janik, W. Li, Selective oxidation of 1,2-propanediol in alkaline anion-exchange membrane electrocatalytic flow reactors: experimental and DFT investigations, ACS Catal. 5 (2015) 6926–6936, doi:10.1021/acscatal.5b01085.

[39] P.S. Fernández, J. Fernandes Gomes, C.A. Angelucci, P. Tereshchuk, C.A. Martins, G.A. Camara, M.E. Martins, J.L.F. Da Silva, G. Tremiliosi-Filho, Establishing a Link between Well-Ordered Pt(100) surfaces and real systems: how do random superficial defects influence the electro-oxidation of glycerol? ACS Catal. 5 (2015) 4227–4236, doi:10.1021/acscatal.5b00451.

[40] D.Z. Jeffery, G.a. Camara, The formation of carbon dioxide during glycerol electrooxidation in alkaline media: first spectroscopic evidences, Electrochem. Commun. 12 (2010) 1129–1132, doi:10.1016/j.elecom.2010.06.001.

[41] C.A. Angelucci, H. Varela, G. Tremiliosi-Filho, J.F. Gomes, The significance of non-covalent interactions on the electro-oxidation of alcohols on Pt and Au in alkaline media, Electrochem. Commun. 33 (2013) 10–13, doi:10.1016/j.elecom.2013.03.039.

[42] E. Sitta, M.A. Nascimento, H. Varela, Complex kinetics, high frequency oscillations and temperature compensation in the electro-oxidation of ethylene glycol on platinum, Phys. Chem. Chem. Phys. 12 (2010) 15195–15206, doi:10.1039/c002574g.

[43] R. Nagao, E. Sitta, H. Varela, Stabilizing nonstationary electrochemical time series, J. Phys. Chem. C. 114 (2010) 22262–22268, doi:10.1021/jp109554r.

[44] M.F. Cabral, R. Nagao, E. Sitta, M. Eiswirth, H. Varela, Mechanistic aspects of the linear stabilization of non-stationary electrochemical oscillations, Phys. Chem. Chem. Phys. (2013) 15, doi:10.1039/c2cp42890c.

[45] M.A. Nascimento, R. Nagao, M. Eiswirth, H. Varela, Coupled slow and fast surface dynamics in an electrocatalytic oscillator: model and simulations, J. Chem. Phys. 141 (2014) 234701, doi:10.1063/1.4903172.